Catal Lett (2009) 129:104–110
DOI 10.1007/s10562-009-9877-2

# Novel $Y_2O_3$ Doped $MnO_x$ Binary Metal Oxides for $NO_x$ Storage at Low Temperature in Lean Burn Condition

**Junhua Li · Wei Li · Lisi Wei · Ralph T. Yang**

Received: 24 December 2008 / Accepted: 22 January 2009 / Published online: 14 February 2009


**Abstract** $MnO_x$-$Y_2O_3$ binary metal oxide catalysts are synthesized by a constant-pH co-precipitation method, their ability of $NO_x$ storage capacity and absorbing process were investigated. The pure $MnO_x$ and $Y_2O_3$ calcined at 500 °C for 4 h in static air are both of body-centre structure, while the binary metal oxides containing Mn and Y are mainly of amorphous phase. The adulteration of $Y_2O_3$ can remarkably improve the specific surface areas of the catalysts, which probably result of the enhancement on NO storage capacity and catalytic oxidation ability of NO at 100 °C. The XPS results indicate that both Mn and Y have 3+ chemical states in the binary oxides. FT-IR spectra could be beneficial to explain the NO storage process on the binary metal oxide: NO can be adsorbed on the $MnO_x$ and $Y_2O_3$ sites as nitrates and nitrites, respectively, and then the nitrites on $Y_2O_3$ site are shifted to $Mn_2O_3$ site and then is oxidized to nitrates. As a result, the NO storage capacity is enhanced due to the adulteration of $Y_2O_3$, finally the $NO_x$ are adsorbed on the $Mn_2O_3$ site as nitrate species.

**Keywords** $NO_x$ · $NO_x$ storage capacity · NSR · $Y_2O_3$ · $Mn_2O_3$ · Binary metal oxide · Lean burn condition

J. Li · W. Li · L. Wei
Department of Environment Science and Engineering, Tsinghua University, Beijing 100084, China

J. Li (✉) · R. T. Yang
Department of Chemical Engineering, University of Michigan, Ann Arbor, MI 48109-2136, USA
e-mail: lijunhua@tsinghua.edu.cn; jhli@umich.edu

## 1 Introduction

The lean-burn engine has attracted more and more attention due to its high fuel economy and low $CO_2$ emission inventory. Three-way catalyst (TWC) is widely applied in gasoline engine operated on stoichiometric conditions; however, it could not effectively remove $NO_x$ in lean-burn conditions [1]. The $NO_x$ storage reduction (NSR) method, brought forward by TOYOTA Company, is a promising way to eliminate $NO_x$ in lean-burn exhaust gas [2–6]. The NSR systems demands a sequence of lean and rich operating periods, which storage $NO_x$ in lean condition and then reduce to $N_2$ in rich condition. Up to now, most of investigations regarding the NSR catalyst were focused on Pt-BaO-$Al_2O_3$ catalysts [7–14], in which Pt could oxidize NO to $NO_2$ in lean-burn condition and reduce $NO_2$ to NO in rich-burn condition, and BaO could work as a storage material.

Although Pt-BaO-$Al_2O_3$ is a potentially commercial NSR catalyst for lean $NO_x$ reduction, it has not been widely used in diesel vehicles due to the narrow temperature window. For example, Pt-BaO-$Al_2O_3$ only show good NSC performance above 300 °C, while the exhaust gas temperature of a light-duty diesel vehicle driving under the Federal test procedure (FTP) is typically less than 200 °C, and the operation temperature window of the conventional NSR ranges from 200 to 500 °C [15]. Therefore, many researchers are continually to develop high NSC materials even at low temperature for real application.

Regarding the $NO_x$ storage reduction at low temperature, $MnO_x$ has been attracted much attention in past decade [16–18]. It is reported that $MnO_x$-$CeO_2$ mixed oxides showed a good NSC at 100–150 °C. When Pd was loaded on this catalyst, $NO_x$ was reduced to $N_2$ at low temperature in the presence of $H_2$. In this work, $Y_2O_3$ doped $MnO_x$ binary metal oxide catalysts with various ratio of Mn/Y were

prepared by co-precipitation method and they showed better NSC at a low temperature. Furthermore, the adsorbing process was investigated through in situ DRIFTS analysis.

## 2 Experimental

### 2.1 Materials Preparation

The binary metal oxide $MnO_x$-$Y_2O_3$ samples were prepared with a constant-pH co-precipitation method where the ratio of Y/Mn was 1/10, 3/10 and 5/10, respectively. These samples were denoted as Mn10Y1, Mn10Y3 and Mn10Y5. For comparison, pure $MnO_x$ and $Y_2O_3$ oxides were prepared similarly, and denoted as Mn10Y0 and Mn0Y10. In brief, a binary salt solution (200 mL) was simultaneously added drop-wise into 200 mL $NH_4HCO_3$ solution within 30 min at constant pH (9–10) under vigorous mechanical stirring. The binary salt solution contained $Mn(CH_3COO)_2$ and $Y(NO_3)_3$ with the designed molar ratio. The $[OH^-]$ of $NH_4HCO_3$ solution was designed to keep 2.5 times of $[Mn^{X/2+}]$. The precipitates were first aged in suspension at room temperature for 4 h while stirring in the static air, and then filtered and thoroughly washed with doubly distilled water. The cake was dried at 90 °C overnight, and then calcined at 500 °C for 4 h to derive Mn-Y-O binary oxide catalysts. The oxide catalysts were then crushed and sized to 40–60 mesh for sorption experiments and kept in a desiccator to avoid water vapor.

### 2.2 Materials Characterization

BET surface area measurements were performed by using $N_2$ adsorption, and the samples were evacuated at 200 °C under vacuum for 4 h. The specific surface area was determined from the linear part of the BET equation.

The X-ray diffraction (XRD) pattern of Mn-Y-O samples was recorded with an Automated D/Max B diffractometer. Cu Kα radiation was utilized in X-ray tube operated at 40 kV and 120 mA.

The X-ray Photoelectron Spectroscopy (XPS) measurements were performed on a PHI-5300/ESCA instrument, using Al/Mg primary radiation (3.0 kV, 25 mA).

In situ DRIFTS spectra were recorded on a NEXUS 670-FTIR. The samples were finely ground and placed in a ceramic crucible. The feed gas streamed into the cell at a total flow rate of 100 mL/min$^{-1}$. The temperature in the cell could be programmed from 20 to 800 °C. Prior to analysis, the samples were heated firstly in $N_2$ and $O_2$ for 60 min. The background spectra were collected after dwelling for 30 min at a desired temperature. The sample spectra reported here were collected after dwelling for 30 min. In all cases, 100 scans were recorded at a resolution of 4 cm$^{-1}$.

### 2.3 $No_x$ Adsorption/Desorption

$NO_x$ Storage Capability (NSC) measurements are carried out in a U-type quartz reactor with an inner diameter of 5 mm under normal atmospheric pressure. A 0.5 g sample was employed in this test. After pretreatment by flowing pure $N_2$ (400 mL/min) at 500 °C for 30 min, the samples were cooled to 100 °C in $N_2$ for adsorption. Then a gas mixture (600 ppm of NO and 8% $O_2/N_2$) was passed through the sample at a space velocity of 48,000 h$^{-1}$ for 30 min. An on-line $NO_x$ analyzer (Cheminulene 42HC) was used to measure the NO-$NO_2$ concentration.

Temperature-programmed desorption (TPD) experiments are carried out in a U-size of fixed-bed reactor with an inner diameter of 5 mm. The temperature is controlled by a programmable temperature controller (CKW-1100). For $NO_x$ adsorption, a 0.5 g sample was first treated with nitrogen at 500 °C for 30 min. After being cooled down to 100 °C, the sample was exposed to the flow of 600 ppm NO and 8% $O_2/N_2$ for 30 min. Then NO and $O_2$ were cut off, pure nitrogen was passed through the reactor, and nitrogen oxides desorption was performed by ramping the temperature from 100 to 600 °C at 10 °C/min. The total flow rate was 400 mL/min.

## 3 Results and Discussion

### 3.1 Effect of Y/Mn Ratios of Binary Metal Oxides

Figure 1 shows the XRD patterns of the binary metal oxide samples with different ratios of Mn. The compound

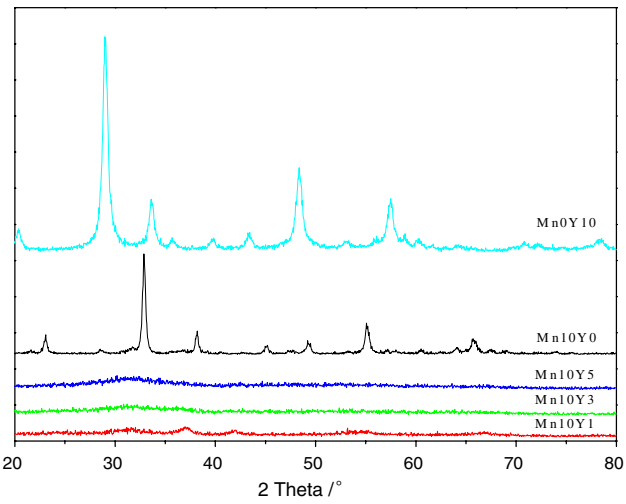


**Fig. 1** XRD patterns of various samples prepared by co-precipitation

Mn10Y0 shows the typical diffraction peaks at 23, 33, 38 and 56°, attributed to the body-centre $Mn_2O_3$ structure; the compound Mn0Y10 shows the typical diffraction peaks at 28, 34, 48 and 57°, attributed to the body-centre $Y_2O_3$ structure; the compounds Mn10Y1, Mn10Y3 and Mn10Y5 show weak diffraction peaks due to the amorphous structure.

The XRD spectra show that inducing $Y_2O_3$ to $MnO_x$ can weaken the crystal intensity of the samples. In addition, the spectrum of the components of Mn10Y1 contains several peaks at 31.6 and 37which are not found in Mn10Y0 and Mn0Y10. This indicates that inducing $Y_2O_3$ to $MnO_x$ could also change the crystal structure of the samples. Considering on the differences in radius between $Mn^{3+}$ and $Y^{3+}$, there would be the lacuna, or the collapse on the crystal structure, of the samples.

The specific surface areas of Mn-Y-O catalysts are summarized in Table 1. It can be seen that both Mn10Y0 and Mn0Y10 samples have very small BET areas, while Mn10Y1, Mn10Y3 and Mn10Y5 samples have much large BET areas. Combined with the XRD spectra, it can be found that inducing $Y_2O_3$ to $MnO_x$ can not only change the crystal structures of the samples, but also influence the BET areas. The catalysts with higher crystal intensity have smaller BET areas. The binary metal oxides with amorphous structure possess large BET areas, which is helpful to improve the absorption ability of the catalysts.

The XPS of Mn10Y1 and Mn10Y3 are shown in Fig. 2. The elements Mn ($Mn3p_{3/2}$, Mn3s, $Mn2p_{1/2}$), Y ($Y3d_{5/2}$) and O (O1s) are analyzed in the range between 0 and 1,000 eV of electron combining energy. Compared with these two samples, the location of each peak has little offset, but the intensity of each peak has a large variance, which is mainly due to the difference in the ratio of Y/Mn.

The peak locations of elements Mn and Y are shown in Table 2. It indicates that each sample containing Mn and Y has the same peak location as $Mn^{3+}$ and $Y^{3+}$. In the spectra each peak is symmetrical without distinct division, which indicates that Mn and Y in the catalysts have only one chemic state, without metal or other states of Mn or Y.

**Table 1** The BET surfaces of various samples

| Samples | BET areas ($m^2$/g) |
|---|---|
| Mn10Y0 | 42.98 |
| Mn10Y1 | 153.4 |
| Mn10Y3 | 151.9 |
| Mn10Y5 | 137.7 |
| Mn0Y10 | 23.89 |

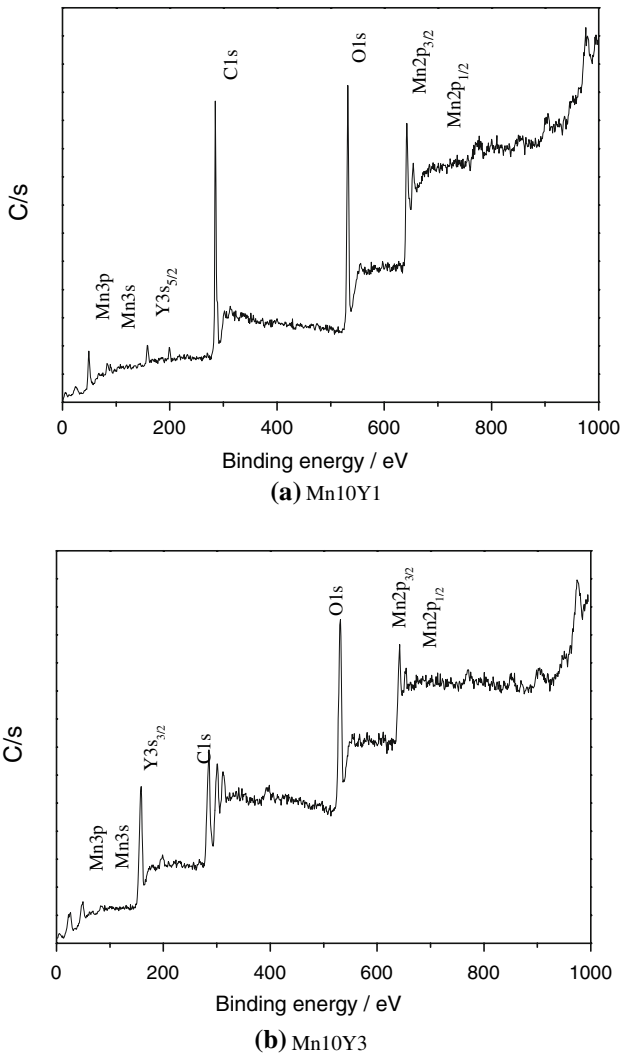


**Fig. 2** XPS spectra of Mn10Y1 and Mn10Y3 samples

**Table 2** The XPS adsorbing peak locations of the samples

| Samples | Peak Location (eV) | | |
|---|---|---|---|
| | $Mn2p_{3/2}$ | $Mn2p_{1/2}$ | $Y3d_{5/2}$ |
| Standard location | 641.7 ($Mn_2O_3$) | 653.7 ($Mn_2O_3$) | 156.9 ($Y_2O_3$) |
| Mn10Y1 | 641.8 | 653.8 | 158.0 |
| Mn10Y3 | 641.7 | 653.4 | 158.0 |

### 3.2 NO Adsorption/Desorption on Binary Metal Oxides

The adsorption profiles of NO on these binary metal oxide catalysts at 100 °C in the presence of $O_2$ are presented in Fig. 3. NO is completely trapped in the initial period (180–720 s) for all catalysts at 100 °C. NO is continuously trapped in the next 600–900 s since NO concentration is gradually recovered to 520–580 ppm. The adulteration of

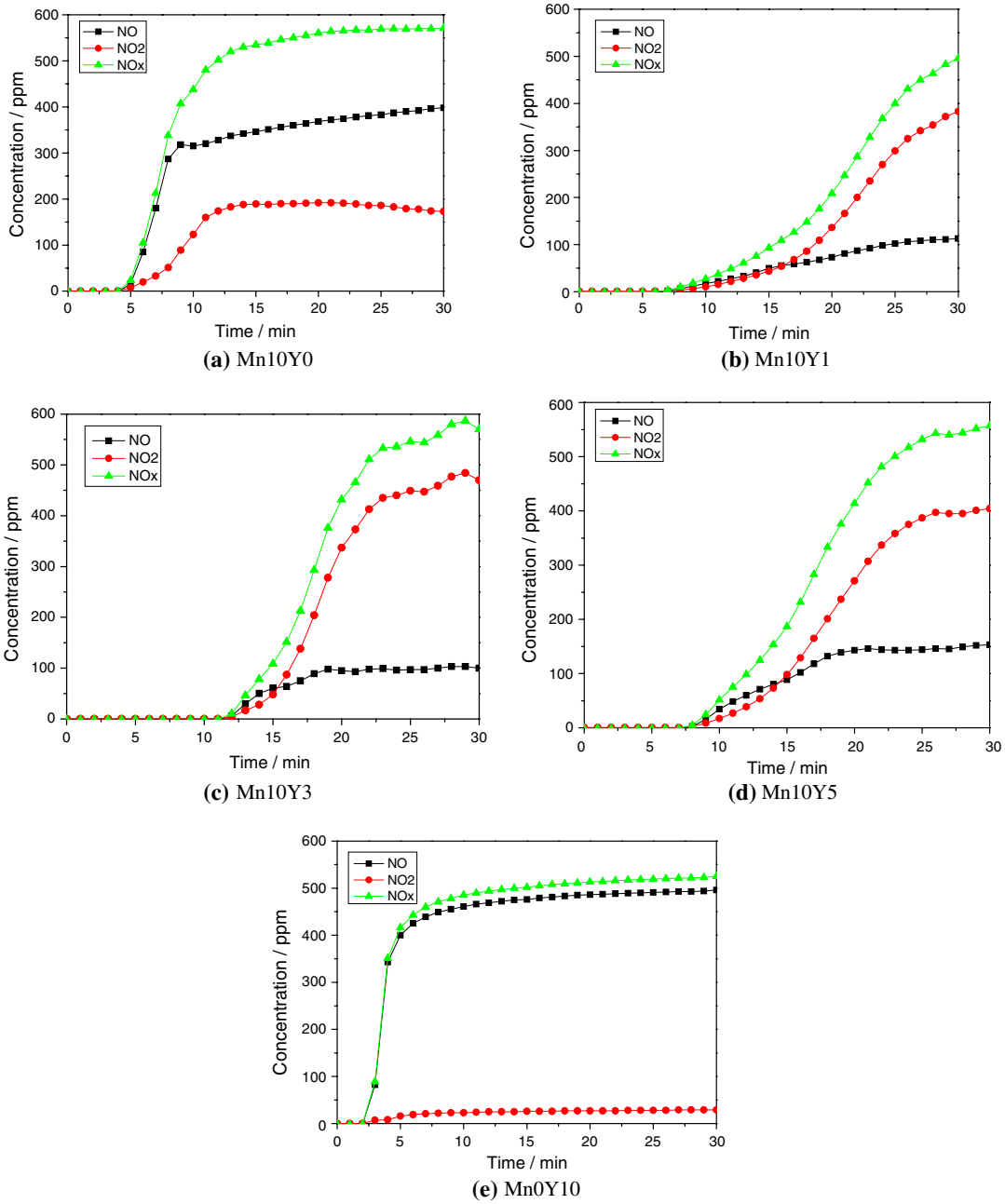


**Fig. 3** NSC profiles of different catalysts at 100 °C in $O_2$. (Reaction conditions: 600 ppm NO, 8% $O_2/N_2$, GHSV = 48,000 $h^{-1}$, pretreated at 500 °C for 30 min in $N_2$)

$Y_2O_3$ could delays the recovery of NO concentration, which increases the storage of NO. The $NO_x$ storage capacities (NSC) of each catalyst are showed in Table 3. It indicates that Mn10Y0 and Mn0Y10 show low storage ability of NO, while Mn10Y1, Mn10Y3 and Mn10Y5 show high NO storage ability. In the Mn0Y10 sample, $NO_2$ in the downstream is found at a very low concentration, less than 40 ppm, demonstrating very limited conversion of NO to $NO_2$ at 100 °C in $O_2$. In the Mn10Y0 sample, $NO_2$ in the downstream is found at a higher concentration, less than

**Table 3** Break time and $NO_x$ storage capacity of the samples under different adsorption conditions at 300 °C

| Samples | Break time (min) | $NO_x$ storage capacity (μmol/g) |
|---|---|---|
| Mn10Y0 | 4 | 107.1 |
| Mn10Y1 | 7 | 358.1 |
| Mn10Y3 | 12 | 333.8 |
| Mn10Y5 | 8 | 302.6 |
| Mn0Y10 | 3 | 117.2 |

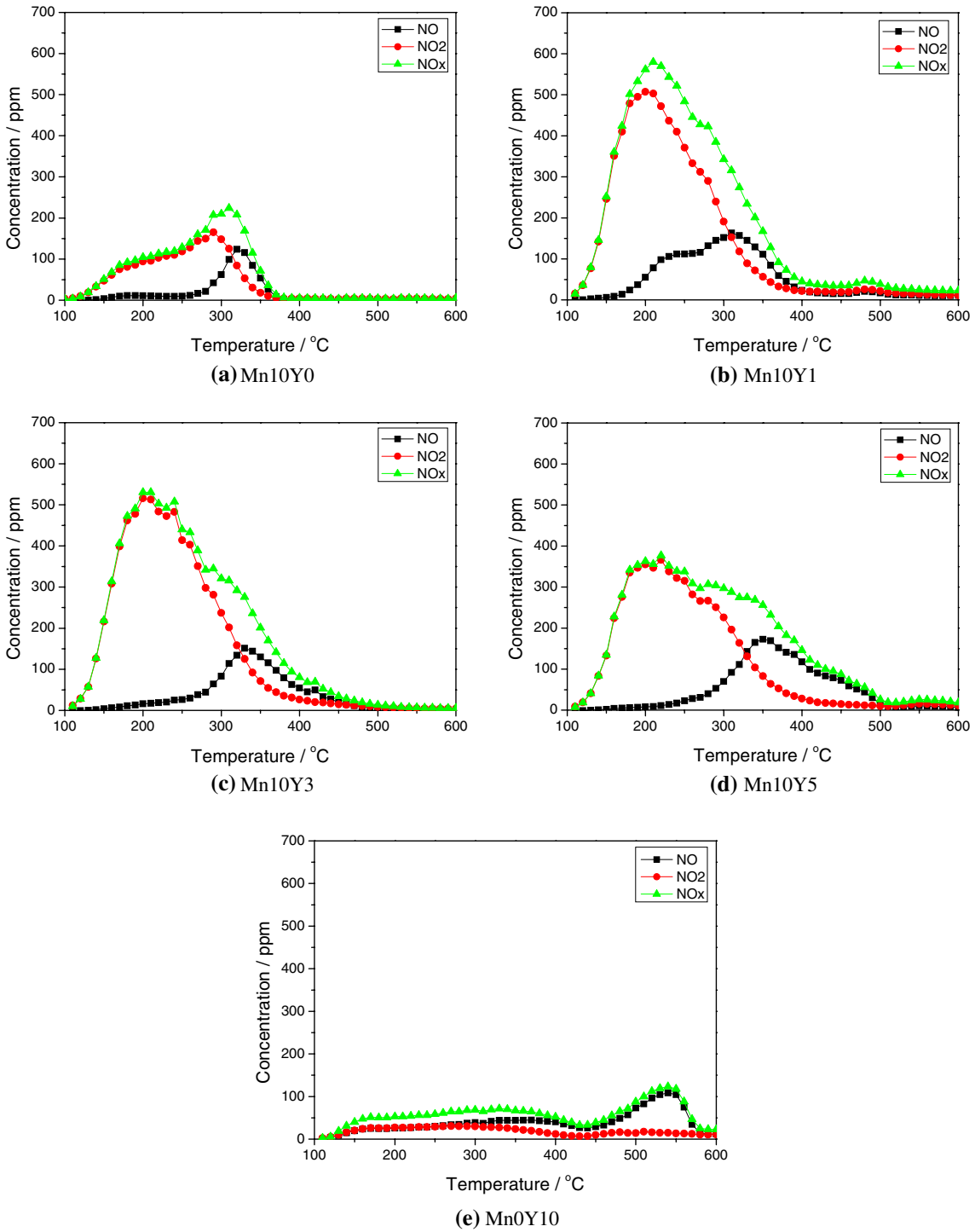


**Fig. 4** NO-TPD profiles of different catalysts prior to co-adsorbing NO and $O_2$ at 100 °C. (Reaction conditions: 600 ppm NO, 8% $O_2/N_2$, GHSV = 30,000 $h^{-1}$, pretreated at 500 °C for 30 min in $N_2$)

200 ppm, and demonstrating higher catalytic oxidation ability. In Mn10Y1, Mn10Y3 and Mn10Y5 samples, $NO_2$ is found at much higher concentration, more than 60% of the $NO_x$ concentration, demonstrating much higher catalytic oxidation ability. Comparing these samples, it can be concluded that the adulteration of $Y_2O_3$ can not only improve the $NO_x$ storage capacity, but also enhance the catalytic oxidation ability of the samples.

Figure 4 shows the results of desorption of $NO_x$ on binary metal oxides, on which NO was previously adsorbed at 100 °C for 30 min, and then was heated from 100 to 600 °C. Each catalyst has one major desorption peak, the

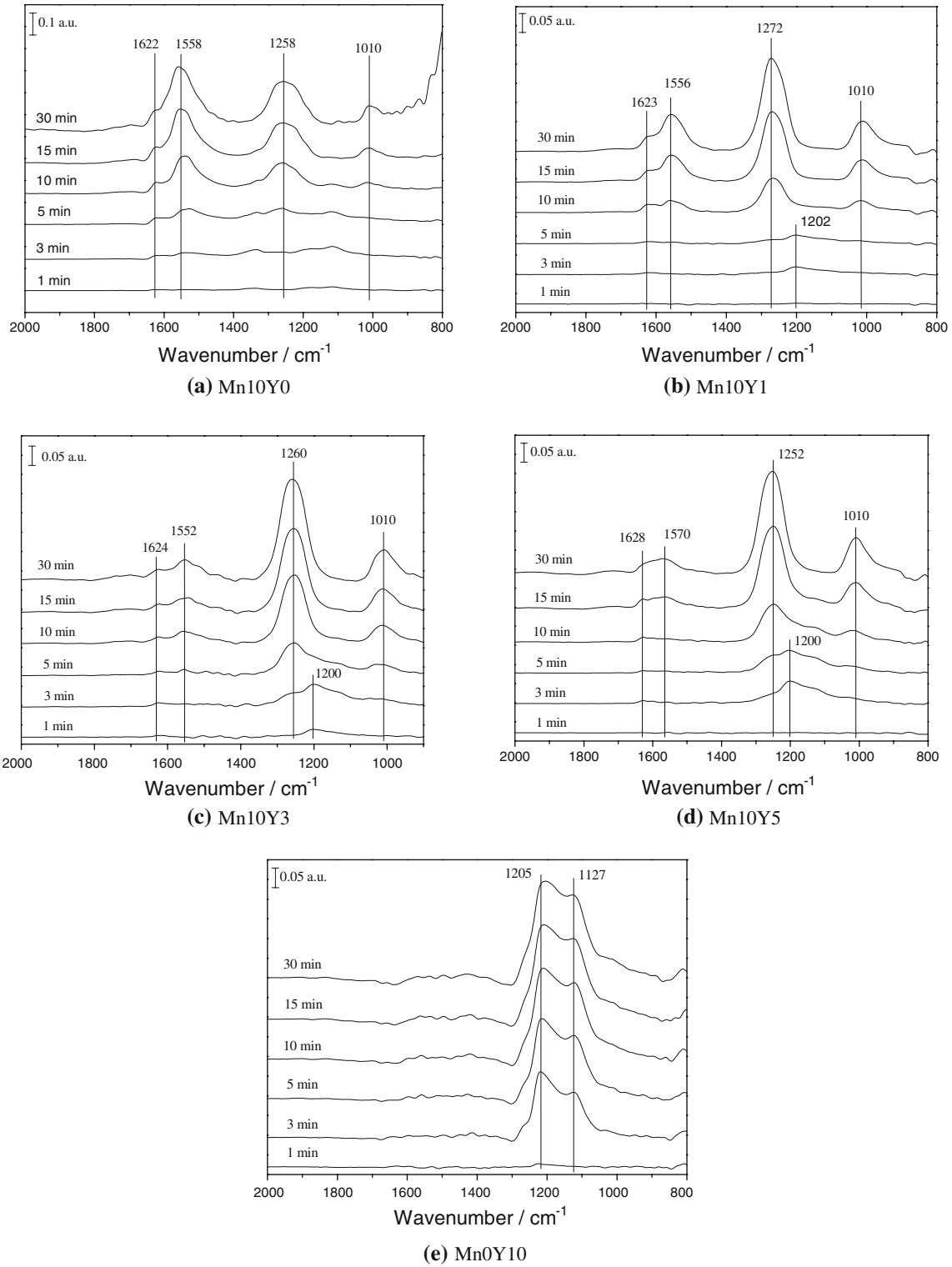


**Fig. 5** FTIR spectra of NO and $O_2$ co-adsorption on various catalysts (Feed gas composition: 600 ppm NO, 8% $O_2$, $N_2$ as the balance gas, pretreated at 500 °C for 30 min in $N_2$)

area of which is equivalent to its NSC data. The peak temperature of Mn0Y10 is at 540 °C, the highest of all, while the peak temperature of Mn10Y1, Mn10Y3 and Mn10Y5 are in the temperature range of 200 and 250 °C, and the peak temperature of Mn10Y0 is at 310 °C. It indicates that the adulteration of $Y_2O_3$ promoted the NO oxidization to $NO_2$ at low temperature, which then results in the increase of $NO_x$ storage. However, the stability of the

nitrates formed on the surface of the catalysts decreased, which is beneficial to $NO_x$ release and reduction in rich condition. The component of the desorption gas correspond to the downstream gas of $NO_x$ storage.

Combined with the XRD and BET data, the pure $MnO_x$ and $Y_2O_3$ both have little $NO_x$ storage capacity and limited NO catalytic oxidation ability, but the adulteration of $Y_2O_3$ to $MnO_x$ could weaken the crystal intensity of the samples and enlarge the BET areas of the samples. Because the sample with larger BET areas contains more NO adsorbing active sites, it is helpful to $NO_x$ storage and NO catalytic oxidation.

### 3.3 NO Adsorption Mechanism on Binary Metal Oxides

The FTIR spectra of $MnO_x$-$Y_2O_3$ samples exposed to 600 ppm NO in $N_2$ and $O_2$ mixture at 100 °C for 30 min are shown in Fig. 5. On the surface of Mn0Y10 catalyst, the adsorbing species are mainly nitrites (1,127 and 1,205 $cm^{-1}$) [19, 20], indicating a weak NO catalytic oxidation ability, which are corresponding to the results of NSC and NO-TPD. On the surface of Mn10Y0, the spectra contain several major peaks between 1,000 and 1,630 $cm^{-1}$, which can be assigned to cis-$(N_2O_2)^{2-}$ (1,010 $cm^{-1}$), $NO_3^-$ (1,258 and 1,558 $cm^{-1}$) and $NO_2$ (1,622 $cm^{-1}$) species [21, 22]. In these spectra they do not show the transformation from nitrites to nitrates, and the species at 1,558 $cm^{-1}$ is the main adsorbing species. On the surface from Mn10Y1, Mn10Y3 and Mn10Y5, the adsorbing species are mainly the same as Mn10Y0, but different from Mn0Y10. However, there are two main differences between these samples and Mn10Y0. One is a transformation from nitrites (1,202 $cm^{-1}$) to nitrates (1,260 $cm^{-1}$), the other is that the main adsorbing species turns to be the $NO_3^-$ species at 1,260 $cm^{-1}$. The nitrites on the species in the first 5 min are at the same location as Mn0Y10, while they are not observed on Mn10Y0. At the end of the NO storage, the species on Mn10Y1, Mn10Y3 and Mn10Y5 are at the same location as Mn10Y0, but not Mn0Y10. These indicates that at the beginning of NO storage, NO is adsorbed on $MnO_x$ and $Y_2O_3$ in the form of nitrates and nitrites, respectively. Then the nitrites on $Y_2O_3$ is shifted to the surface of $MnO_x$ and oxidized to nitrates. The presence of $Y_2O_3$ could not only enlarge the BET surface areas of samples, but also served to adsorb NO as nitrites so as to improve the $NO_x$ storage ability.

## 4 Conclusions

$Y_2O_3$ doped $MnO_x$ binary metal oxides show high $NO_x$ storage capacities and catalytic oxidation ability of NO to $NO_2$ at low temperature due to their amorphous configuration and high specific surface areas. The XPS results indicate that both Mn and Y have 3+ chemical states in the binary oxides. Based on the DRIFTS results, NO is adsorbed on the $MnO_x$ and $Y_2O_3$ sites as nitrates and nitrites, respectively, and then the nitrites on $Y_2O_3$ site are shifted to $Mn_2O_3$ site and oxidized to nitrates.

**Acknowledgments** The work was financially supported by National Natural Science Fund of China (Grant No. 20677034), and the National High-Tech Research and Development (863) Program of China (Grant No. 2006AA060301), and New Century Excellent Talents in University of China (NCET-2005).

## References

1. Farrauto RJ, Heck RM (1999) Catal Today 51:351
2. Takahashi N, Shinjoh H, Iijima T, Suzuki T, Yamazaki K, Yokota K, Suzuki H, Miyoshi N, Matsumoto S, Tanizawa T, Tanaka T, Tateishi S, Kasahara K (1996) Catal Today 27:63
3. Matsumoto S, Ikeda Y, Suzuki H, Ogai M, Miyoshi N (2000) Appl Catal B 25:115
4. Kašpar J, Fornasiero P, Hickey N (2003) Catal Today 77:419
5. Li JH, Li W, Kang SF, Ke R (2007) Catal Lett 116:155
6. Wei LS, Li JH, Tang XF (2009) Catal Lett 127:107
7. Castoldi L, Nova I, Lietti L, Forzatti P (2004) Catal Today 96:43
8. Nova I, Castoldi L, Lietti L, Tronconi E, Forzatti P (2002) Catal Today 75:431
9. . Wei XY, Liu XS, Deeba M (2005) Appl Catal B 58:41
10. Liu Zh Q, Anderson JA (2004) J Catal 224:18
11. Kabin KS, Muncrief RL, Harold MP (2004) Catal Today 96:79
12. Sedlmair C, Seshan K, Jentys A, Lercher JA (2002) Catal Today 75:413
13. Cant NW, Patterson MJ (2002) Catal Today 73:271
14. Frola F, Manzoli M, Prinetto F, Ghiotti GJ (2008) Phys Chem C 112:12869
15. Xu L, Graham G, McCabe R (2007) Catal Lett 115:108
16. Koichi E, Takashi K, Tomio H, Hiromichi A (1998) Appl Catal B 16:69
17. Machida M (2002) Catal Surv Jpn 5:91
18. Machida M, Kurogi D, Kijima T (2003) Catal Today 84:201
19. Hadjiivanov K, Saussey J, Freysz JL, Lavalley JC (1998) Catal Lett 52:103
20. Hadjiivanov K, Knözinger H (2000) Phys Chem Chem Phys 2:2803
21. Su Y, Amiridis MD (2004) Catal Today 96:31
22. Su Y, Kabin KS, Harold MP, Amiridis MD (2007) Appl Catal B 71:207